Science Advances
AAAS

advances.sciencemag.org/cgi/content/full/6/47/eabc6457/DC1

Supplementary Materials for

Network-based atrophy modeling in the common epilepsies: A worldwide ENIGMA study

Sara Larivière, Raúl Rodríguez-Cruces, Jessica Royer, Maria Eugenia Caligiuri, Antonio Gambardella, Luis Concha, Simon S. Keller, Fernando Cendes, Clarissa Yasuda, Leonardo Bonilha, Ezequiel Gleichgerrcht, Niels K. Focke, Martin Domin, Felix von Podewills, Soenke Langner, Christian Rummel, Roland Wiest, Pascal Martin, Raviteja Kotikalapudi, Terence J. O'Brien, Benjamin Sinclair, Lucy Vivash, Patricia M. Desmond, Saud Alhusaini, Colin P. Doherty, Gianpiero L. Cavalleri, Norman Delanty, Reetta Kälviäinen, Graeme D. Jackson, Magdalena Kowalczyk, Mario Mascalchi, Mira Semmelroch, Rhys H. Thomas, Hamid Soltanian-Zadeh, Esmaeil Davoodi-Bojd, Junsong Zhang, Matteo Lenge, Renzo Guerrini, Emanuele Bartolini, Khalid Hamandi, Sonya Foley, Bernd Weber, Chantal Depondt, Julie Absil, Sarah J. A. Carr, Eugenio Abela, Mark P. Richardson, Orrin Devinsky, Mariasavina Severino, Pasquale Striano, Domenico Tortora, Sean N. Hatton, Sjoerd B. Vos, John S. Duncan, Christopher D. Whelan, Paul M. Thompson, Sanjay M. Sisodiya, Andrea Bernasconi, Angelo Labate, Carrie R. McDonald, Neda Bernasconi, Boris C. Bernhardt*

*Corresponding author. Email: boris.bernhardt@mcgill.ca

Published 18 November 2020, *Sci. Adv.* **6**, eabc6457 (2020)
DOI: 10.1126/sciadv.abc6457

This PDF file includes:

SUPPLEMENTARY MATERIALS

TABLE S1. **ENIGMA Epilepsy Working Group demographics**. Site-specific demographic breakdown of patient-specific subcohorts, including age (in years), age at onset of epilepsy (in years), sex, side of seizure focus (TLE patients only), and mean duration of illness (in years). TLE=Temporal lobe epilepsy, IGE=idiopathic/genetic generalized epilepsy, HC=healthy controls.

Site name	Case-controls subcohorts		Age (mean±SD)	Age at onset (mean±SD)	Sex (male/female)	Side of focus (L/R)	Duration of illness (mean±SD)
BERN	TLE	*n*=18	31.28±9.09	–	9/9	10/8	–
	IGE	*n*=12	33.03±10.28	–	6/6	–	–
	HC	*n*=76	32.53±9.45	–	35/41	–	–
BONN	TLE	*n*=105	40.28±12.87	17.15±11.95	48/57	69/36	23.12±14.25
	IGE	*n*=0	–	–	–	–	–
	HC	*n*=77	40.12±13.40	–	37/40	–	–
BRUSSELS	TLE	*n*=15	38.13±7.80	11.78±9.92	6/9	11/4	26.43±14.63
	IGE	*n*=8	30.87±11.58	16.37±9.88	2/6	–	14.50±14.73
	HC	*n*=44	26.64±4.33	–	20/24	–	–
CUBRIC	TLE	*n*=0	–	–	–	–	–
	IGE	*n*=44	27.61±7.39	12.95±4.67	12/32	–	14.61±10.03
	HC	*n*=48	28.04±8.17	–	14/34	–	–
EPICZ	TLE	*n*=46	39.70±9.11	18.06±14.15	20/26	19/27	21.63±13.48
	IGE	*n*=0	–	–	–	–	–
	HC	*n*=113	38.38±10.55	–	55/58	–	–
EPIGEN_3.0	TLE	*n*=13	40.39±6.28	21.84±13.16	7/6	8/5	18.55±11.98
	IGE	*n*=0	–	–	–	–	–
	HC	*n*=70	34.75±9.37	–	40/30	–	–
FLORENCE	TLE	*n*=1	41.0	25.0	1/0	1/0	16.0
	IGE	*n*=5	23.40±4.69	10.40±6.66	1/4	–	12.20±6.10
	HC	*n*=14	35.28±8.48	–	6/8	–	–
GREIFSWALD	TLE	*n*=0	–	–	–	–	–
	IGE	*n*=38	41.50±14.39	27.13±16.97	18/20	–	14.37±12.89
	HC	*n*=98	26.48±7.11	–	38/60	–	–
IDIBAPS-HCP	TLE	*n*=53	37.38±9.94	17.73±12.79	24/29	17/36	18.76±9.97
	IGE	*n*=3	38.33±3.51	–	2/1	–	–
	HC	*n*=52	33.13±5.99	–	23/29	–	–
KCL_CNS	TLE	*n*=15	41.90±9.57	17.54±14.16	4/11	6/9	25.17±16.97
	IGE	*n*=32	30.72±9.39	12.12±5.68	11/21	–	18.59±9.54
	HC	*n*=101	31.68±8.40	–	47/54	–	–
KCL_CRF	TLE	*n*=5	37.80±11.52	22.60±12.34	4/1	3/2	15.20±8.04
	IGE	*n*=4	24.50±7.85	23.25±5.74	1/3	–	1.25±2.50
	HC	*n*=26	28.73±8.29	–	10/16	–	–
KUOPIO	TLE	*n*=9	41.11±11.06	23.33±18.23	4/5	0/9	17.78±17.02
	IGE	*n*=35	27.86±8.34	17.46±9.93	13/22	–	10.46±10.67
	HC	*n*=67	25.16±1.55	–	34/33	–	–

Site name	Case-controls subcohorts		Age (mean±SD)	Age at onset (mean±SD)	Sex (male/female)	Side of focus (L/R)	Duration of illness (mean±SD)
MNI	TLE	*n*=82	33.82±10.63	17.37±10.63	35/47	45/37	16.45±11.34
	IGE	*n*=0	–	–	–	–	–
	HC	*n*=46	30.74±7.38	–	25/21	–	–
NYU	TLE	*n*=19	33.84±9.31	14.10±8.04	7/12	8/11	20.21±14.44
	IGE	*n*=36	33.03±9.88	14.28±5.05	20/16	–	19.78±10.83
	HC	*n*=115	30.00±10.43	–	55/60	–	–
RMH	TLE	*n*=32	39.50±12.32	25.83±14.40	19/13	19/13	13.53±13.21
	IGE	*n*=21	31.33±8.79	22.28±9.43	8/13	–	9.51±13.81
	HC	*n*=23	33.96±13.28	–	14/9	–	–
TUBINGEN EKUT_A	TLE	*n*=46	39.70±9.11	18.06±14.15	20/26	19/27	21.63±13.48
	IGE	*n*=0	–	–	–	–	–
	HC	*n*=113	38.38±10.55	–	55/58	–	–
TUBINGEN EKUT_B	TLE	*n*=0	–	–	–	–	–
	IGE	*n*=0	–	–	–	–	–
	HC	*n*=18	35.33±12.28	–	9/9	–	–
UCSD	TLE	*n*=22	37.68±11.17	14.80±12.70	10/12	14/8	24.20±15.74
	IGE	*n*=0	–	–	–	–	–
	HC	*n*=36	35.92±14.09	–	20/16	–	–
UNAM	TLE	*n*=20	34.40±12.47	15.50±13.83	8/12	10/10	18.85±13.83
	IGE	*n*=0	–	–	–	–	–
	HC	*n*=34	33.68±12.15	–	9/25	–	–
UNICAMP	TLE	*n*=191	42.74±8.33	11.39±9.60	78/113	107/84	31.35±12.13
	IGE	*n*=40	33.90±10.67	12.50±8.85	10/30	–	21.20±10.64
	HC	*n*=398	34.39±10.47	–	149/249	–	–
XMU	TLE	*n*=40	28.25±8.45	17.18±12.06	25/15	25/15	11.28±8.02
	IGE	*n*=11	21.00±10.45	18.56±16.49	7/4	–	12.00±10.23
	HC	*n*=13	31.54±6.99	–	9/4	–	–

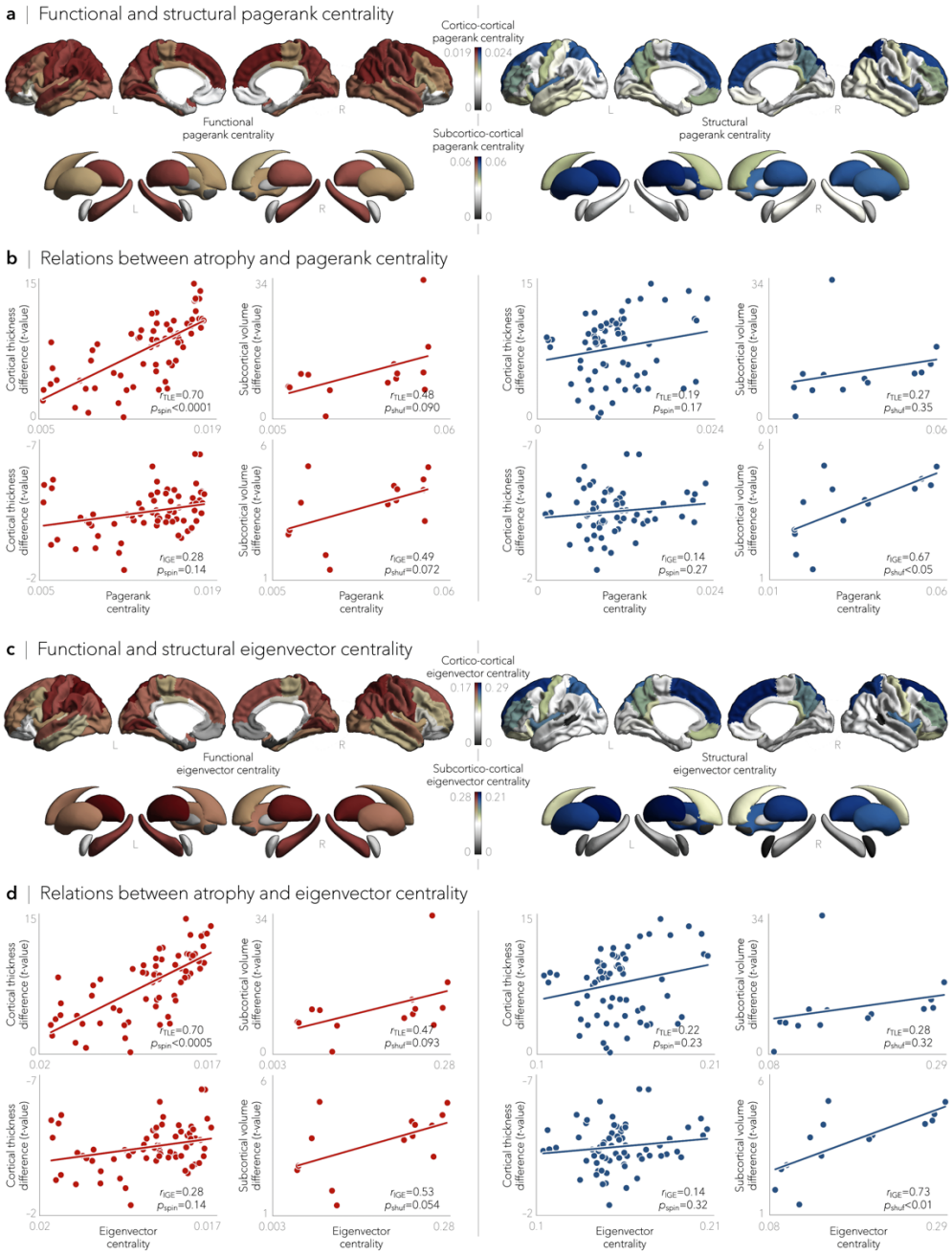

FIGURE S1. **Epilepsy-related atrophy relates to pagerank centrality and eigenvector centrality**. **a** | Normative functional (*left*) and structural (*right*) pagerank centrality, derived from the HCP dataset, was used to identify hubs. **b** | Morphological abnormalities across the common epilepsies related to node-level functional and structural pagerank centrality, with greater atrophy observed in hub regions. Stratifying findings across epilepsy syndromes, we observed a stronger association between cortico-cortical functional hubs and cortical thinning patterns in TLE (p_{spin}<0.0001) and between subcortical volume loss and subcortico-cortical structural hubs in IGE (p_{shuf}<0.05). **c** | Normative functional (*left*) and structural (*right*) eigenvector centrality, derived from the HCP dataset, was also used to identify hubs. **d** | Morphological abnormalities across the common epilepsies related to node-level functional and structural eigenvector centrality, with greater atrophy observed in hub regions. Stratifying findings across epilepsy syndromes, we observed a stronger association between cortico-cortical hubs and cortical thinning patterns in TLE (p_{spin}<0.0005) and between subcortical volume loss and subcortico-cortical hubs in IGE (p_{shuf}<0.01).

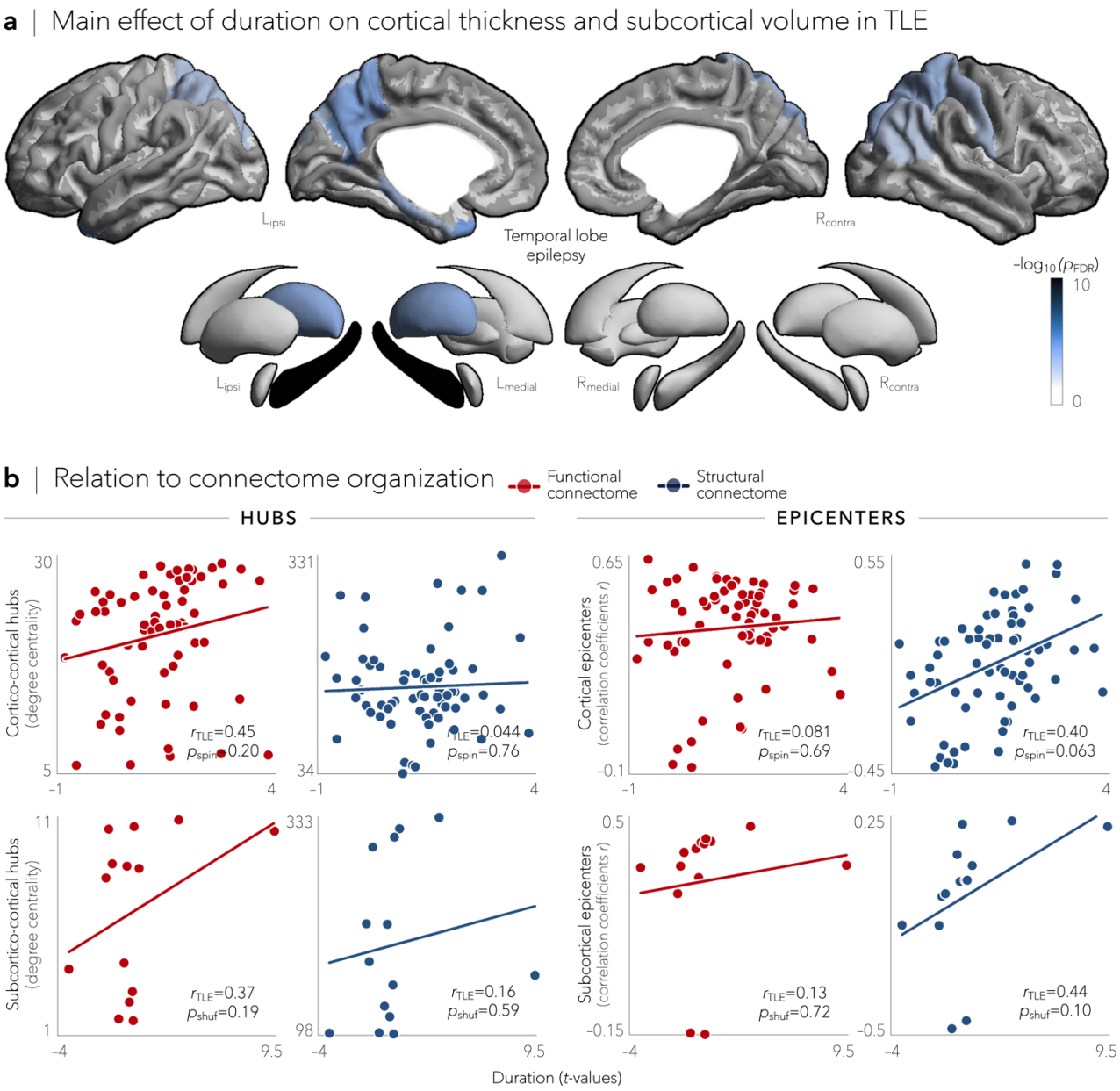

FIGURE S2. Effects of disease duration on cortical thickness and subcortical volume in TLE. a | Main effect of duration of epilepsy on cortical thickness and subcortical volume in TLE; significant negative main effect of duration on atrophy in ipsilateral mesiotemporal cortex ($p_{FDR}<0.005$) and precuneus ($p_{FDR}<2\times10^{-4}$), contralateral postcentral gyrus ($p_{FDR}<0.005$), bilateral superior parietal cortex ($p_{FDR}<7\times10^{-4}$), as well as ipsilateral hippocampus ($p_{FDR}<4\times10^{-20}$) and thalamus ($p_{FDR}<3\times10^{-4}$). Negative $\log_{10}$-transformed FDR-corrected *p*-values are shown. **b** | Scatter plots depict relationships between duration-related effects and functional (*red*) and structural (*red*) degree centrality (*left*) and disease epicenter (*right*); no significant association was observed between connectome organization and indices of disease progression in TLE.

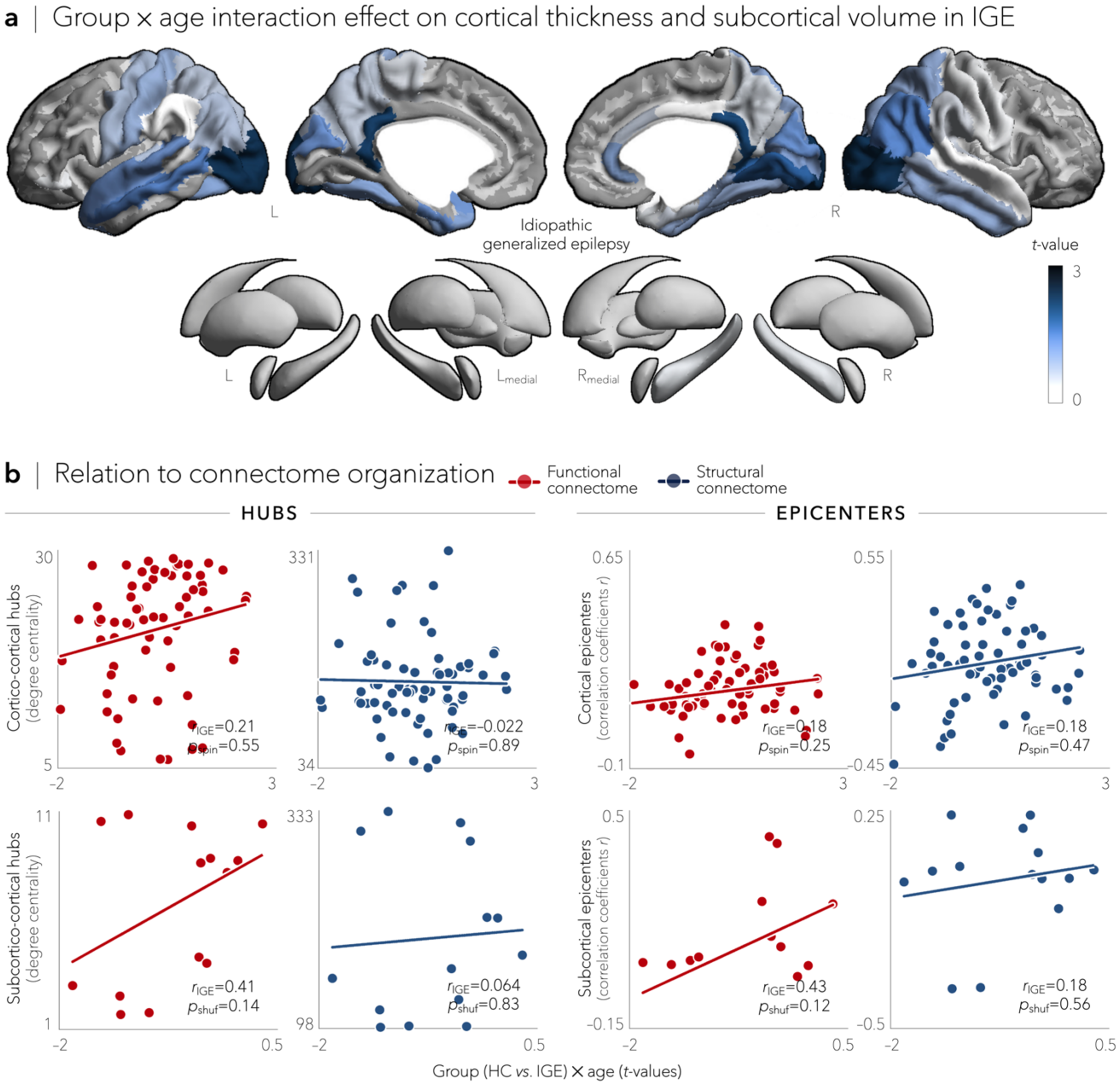

FIGURE S3. **Effects of aging on cortical thickness and subcortical volume in IGE**. **a** | *t*-values for the group (IGE *vs*. HC) × age interaction effect on morphological measures. Findings did not survive significance testing, however, a subtle trend towards negative effects of aging on cortical thickness was observed in bilateral visual (p_{uncorr}<0.05) and posterior cingulate (p_{uncorr}<0.05) cortices. **b** | Scatter plots depict relationships between age-related effects and functional (*red*) and structural (*blue*) degree centrality (*left*) and disease epicenter (*right*); no significant association was observed between connectome organization and indices of disease progression in IGE.

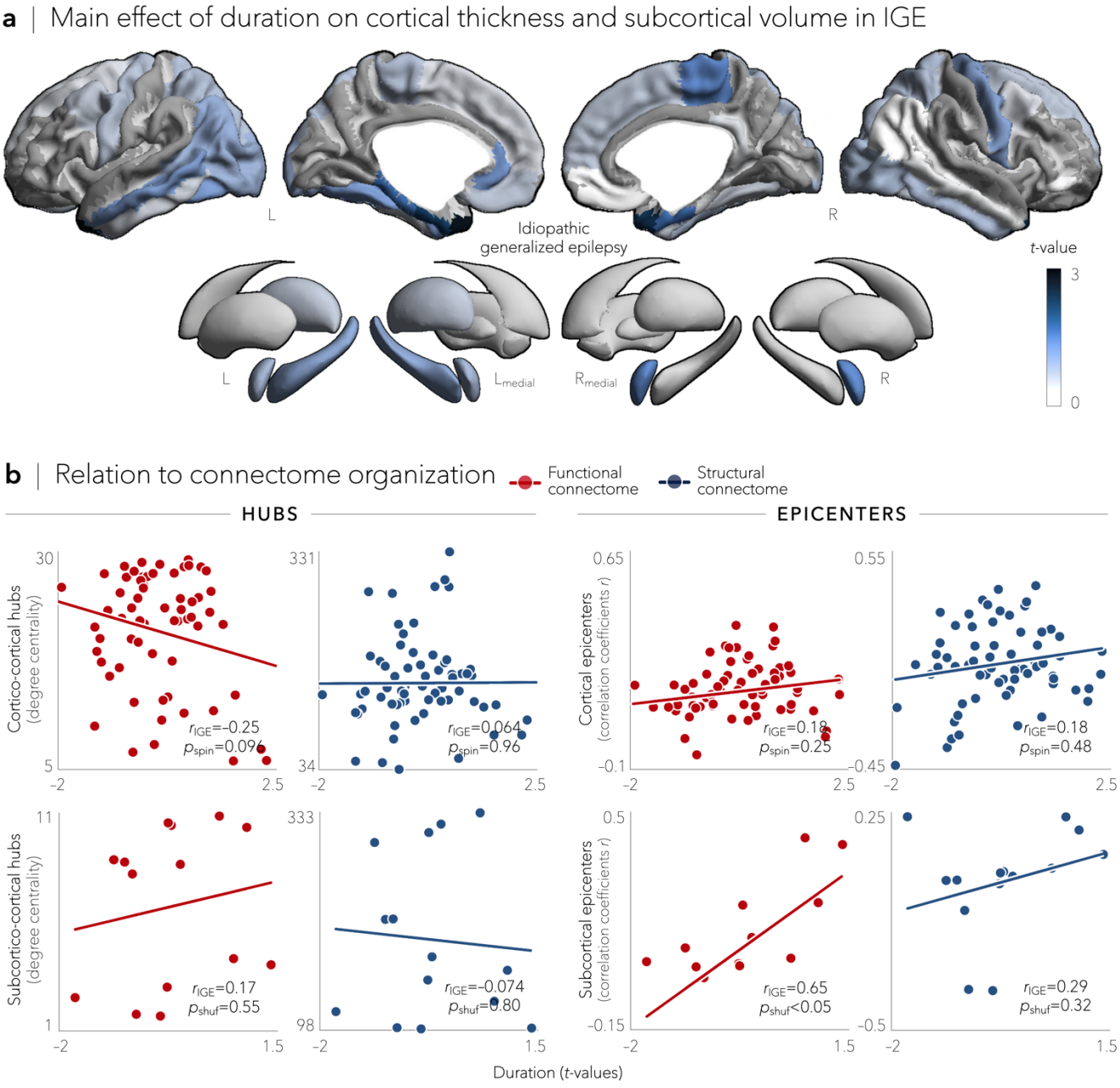

FIGURE S4. Effects of disease duration on cortical thickness and subcortical volume in IGE. a | *t*-values of the main effect of duration of epilepsy on cortical thickness and subcortical volume. Findings did not survive significance testing; subtle trends indicated a negative effect of duration on atrophy in bilateral mesiotemporal regions (p_{uncorr}<0.05), left paracentral cortex (p_{uncorr}<0.1), and right amygdala (p_{uncorr}<0.1). **b** | Scatter plots depict relationships between duration-related effects and functional (*red*) and structural (*blue*) degree centrality (*left*) and disease epicenter (*right*); a significant association was observed between subcortical functional epicenters and duration-related effects in IGE (p_{shuf}<0.05).

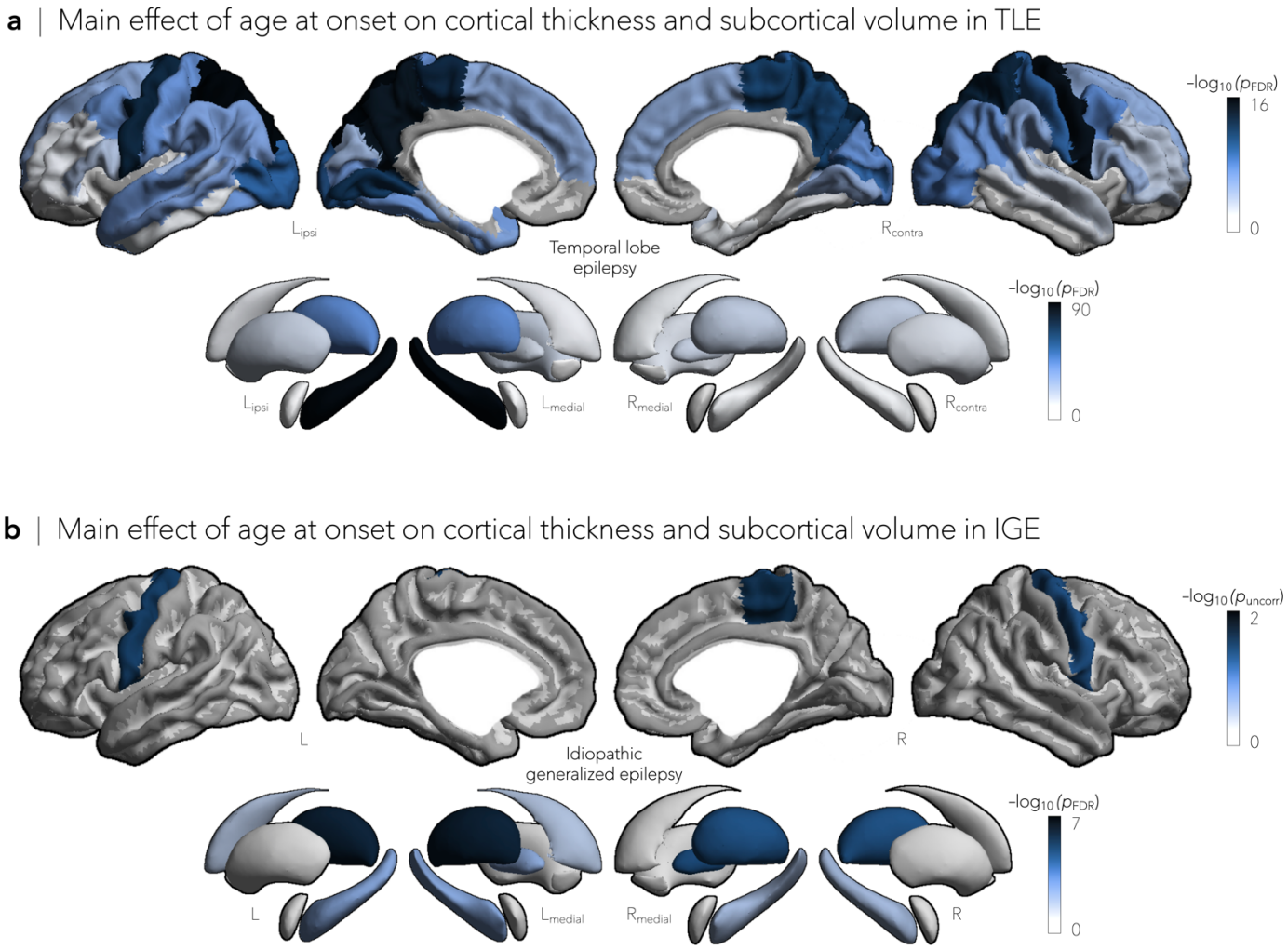

FIGURE S5. **Effects of age at onset on cortical thickness and subcortical volume**. **a** | Negative effects of age at onset on cortical thickness in TLE predominantly affected bilateral precentral ($p_{FDR}<6\times10^{-14}$), superior parietal ($p_{FDR}<6\times10^{-14}$), paracentral ($p_{FDR}<6\times10^{-12}$), precuneus ($p_{FDR}<5\times10^{-12}$), and ipsilateral temporal ($p_{FDR}<2\times10^{-7}$) cortices. Effects of age at onset on subcortical volume reductions were also observed in ipsilateral hippocampus ($p_{FDR}<2\times10^{-86}$) and thalamus ($p_{FDR}<6\times10^{-44}$). **b** | Negative effects of age at onset on cortical thickness and subcortical volume in IGE were mild and mainly targeted bilateral precentral ($p_{uncorr}<0.05$) and left paracentral ($p_{uncorr}<0.05$) cortices. Profound effects of age at onset on subcortical volume reductions was observed in bilateral thalamus ($p_{FDR}<3\times10^{-6}$) and hippocampus ($p_{FDR}<0.01$). Negative $\log_{10}$-transformed FDR-corrected *p*-values are shown.

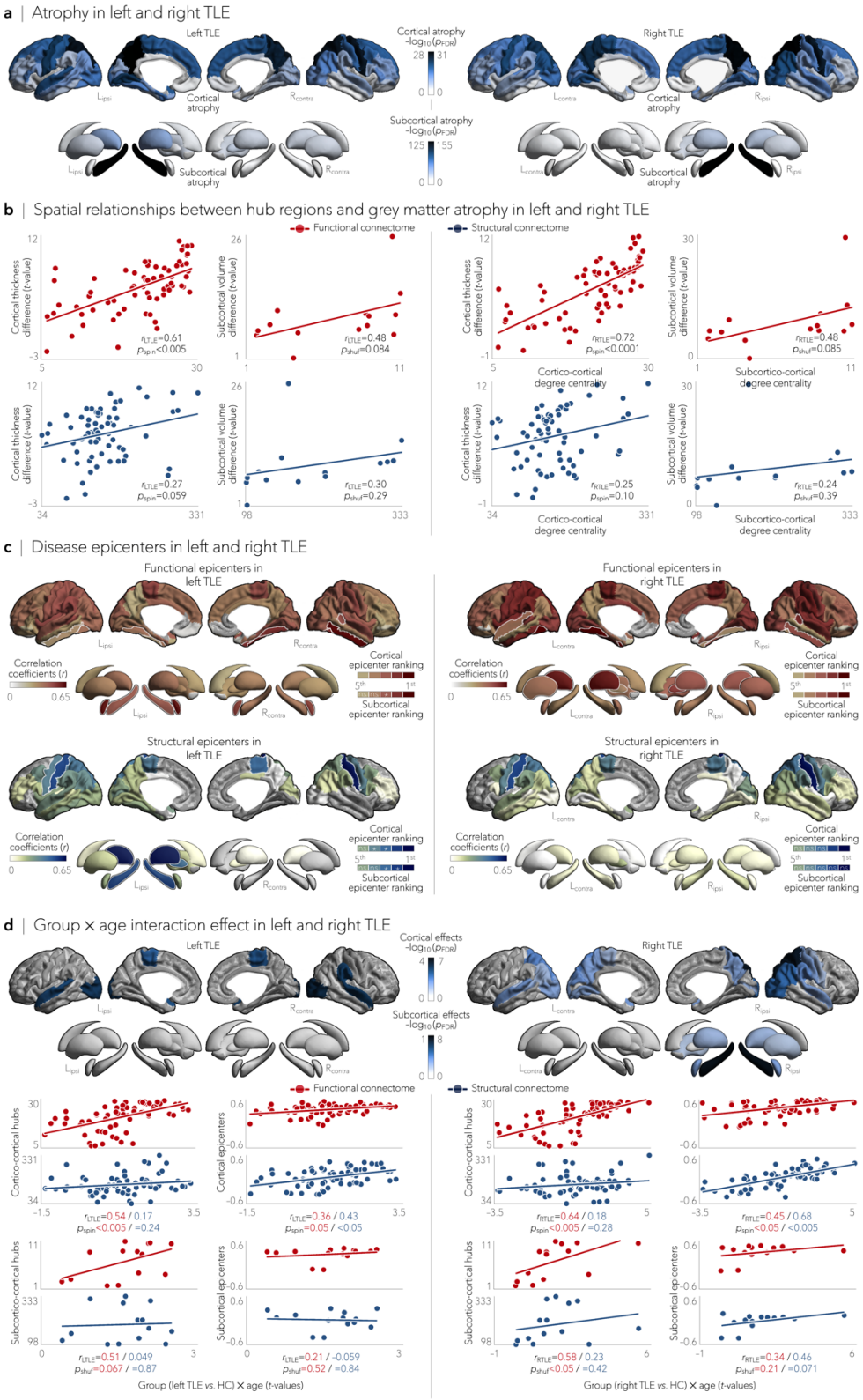

FIGURE S6. Atrophy modelling in left and right TLE. a | Cortical thickness and subcortical volume reductions in left (n=391) and right (n=341) temporal lobe epilepsy (TLE), compared to healthy controls (n=1,418). Left TLE displayed a more widespread distribution of grey matter atrophy than right TLE, particularly affecting ipsilateral

temporal and mesiotemporal cortices ($p_{FDR}<2\times10^{-15}$), as well as bilateral thalamus $p_{FDR}<6\times10^{-23}$). **b** | This distinct pattern of structural abnormalities did not impact the relationship between atrophy and hub distribution; both left and right TLE patients showed significant associations between functional cortico-cortical hubs and atrophy patterns ($p_{spin}<0.005$). **c** | Similar disease epicenters were identified in left and right TLE, with the exception of the ipsilateral hippocampus in left TLE. **d** | Negative effects of age on morphological measures were more pronounced in right, relative to left, TLE, particularly affecting ipsilateral cortical atrophy in superior parietal cortex ($p_{FDR}<0.01$) as well as hippocampal ($p_{FDR}<3\times10^{-8}$), amygdala ($p_{FDR}<0.001$), and thalamic ($p_{FDR}<0.005$) volume. Associations between age-related effects and hub and disease epicenter distributions, however, remained virtually identical across left and right TLE.

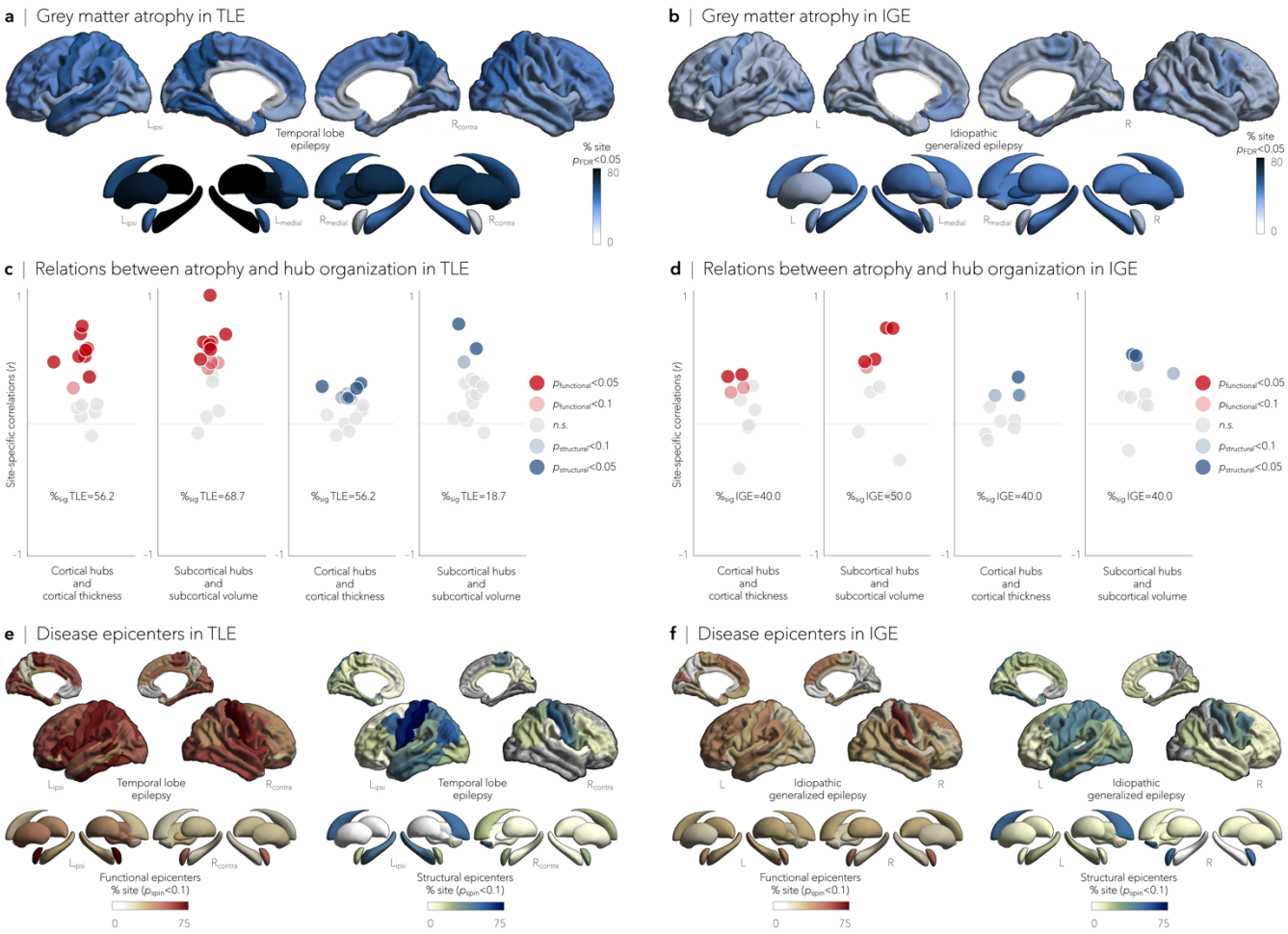

FIGURE S7. Site-specific atrophy modelling. Group-level atrophy modelling analyses were repeated in each site independently and yielded virtually identical results. **a** | In TLE, bilateral fronto-parietal cortical regions and ipsilateral (left) hippocampus and thalamus showed significant atrophy in the majority of sites. **b** | In IGE, bilateral sensorimotor cortices and thalamus were the most consistently atrophied regions across sites. **c** | In TLE, spatial comparisons of hub distribution with atrophy maps yielded consistent findings across sites for both functional (*red*) and structural (*blue*) connectome-derived measures. **d** | Associations between degree centrality (used to identify hub regions) and atrophy maps were observed across individual sites in IGE, with correlations between functional and structural subcortical hubs and subcortical volume reductions being most stable. **e** | Consistent with our main findings, disease epicenters in TLE most consistently emerged in ipsilateral temporo-limbic and subcortical regions. **f** | Disease epicenters in IGE were most often identified in bilateral fronto-central cortices and subcortical structures.

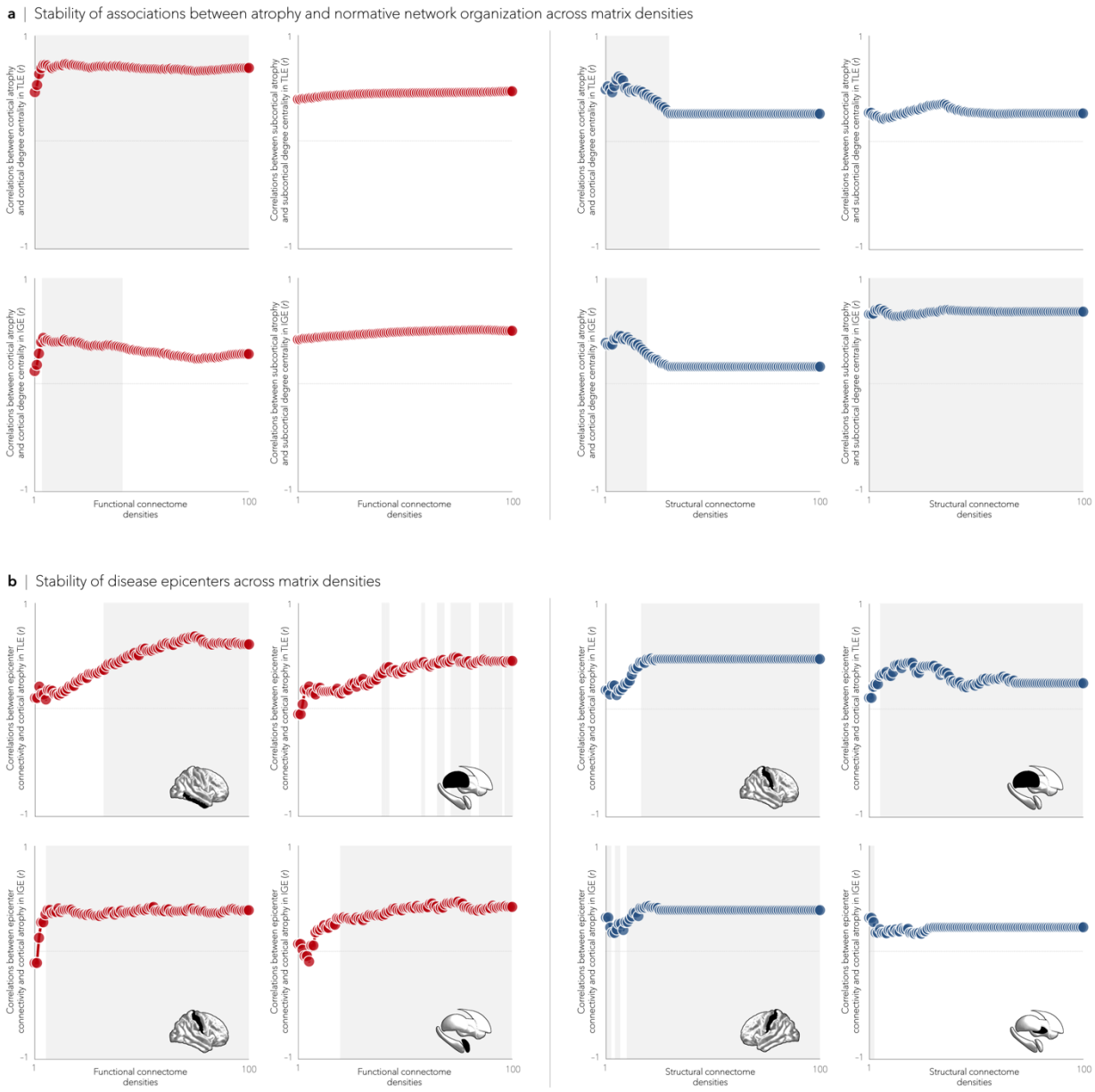

FIGURE S8. **Reproducibility of findings across matrix densities**. **a** | Associations between morphological abnormalities and node-level functional and structural degree centrality across matrix thresholds. In TLE, correlations between cortical atrophy and functional cortico-cortical hubs showed the highest stability, whereas in IGE, correlations between subcortical volume and structural subcortico-cortical hubs showed the highest stability. **b** | Associations between highest ranked functional and structural epicenters' connectivity profiles and epilepsy-related cortical atrophy across matrix thresholds. Correlations between epicenter-based connectivity and atrophy maps were consistent across the majority of thresholds in TLE and IGE. Epicentral regions are shown in inset. Shaded area indicates significant correlations (p_{spin}<0.05).

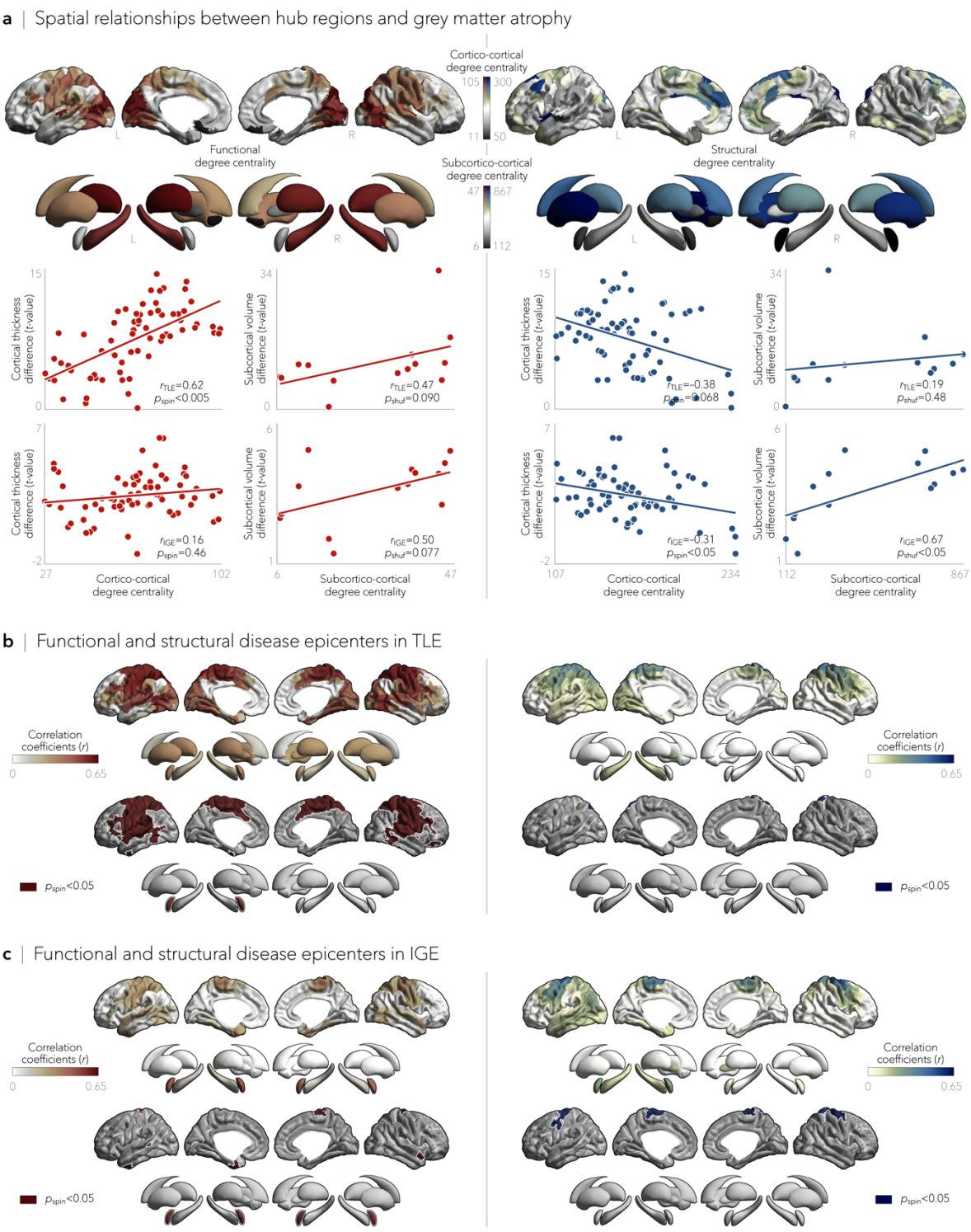

FIGURE S9. **Reproducibility of findings using a higher resolution cortical parcellation**. **a** | Relationships between morphological abnormalities and node-level functional and degree centrality parcellated from Schafer 400. Significant associations were observed between cortical atrophy and functional cortico-cortical hubs in TLE (p_{spin}<0.005) and between subcortical volume and structural subcortico-cortical hubs in IGE (p_{spin}<0.05). **b** | Disease epicenters revealed using functional and structural connectivity mapped to Schaefer 400 *(32)* In TLE, significant functional epicenters

emerged in bilateral temporo-and sensorimotor cortices, and ipsilateral amygdala (p_{spin}<0.005). **c** | In IGE, structural disease epicenters emerged in bilateral fronto-central areas (p_{spin}<0.005).